Bioinorganic Chemistry

The First All-Cyanide Fe_4S_4 Cluster: $[Fe_4S_4(CN)_4]^{3-}$**

*Thomas A. Scott and Hong-Cai Zhou**

In pervasiveness of occurrence and multiplicity of function, iron–sulfur clusters rival the biological prosthetic groups such as hemes and flavins.[1] Starting from the first spontaneous self-assembly of the $[Fe_4S_4(SR)_4]^{2-}$ cluster in 1972,[2] and the identification of the protein-bound Fe_4S_4 in the same year, the study of iron–sulfur clusters has evolved into a mature field in which the synthetic inorganic chemistry now resembles the total synthesis of natural products in organic chemistry.[3] However, the identification of an all-ferrous $Fe_4S_4^0$ state in the Fe protein of nitrogenase,[4,5] which may have important implications in the mechanism of nitrogen fixation,[6,7] has posed a great challenge to inorganic synthetic chemists because when isolated from the protein environment, the $Fe_4S_4^0$ state is difficult to access chemically. For example, the midpoint potential of $[Fe_4S_4(SPh)_4]^{3-/4-}$ is -1.72 V versus saturated calomel electrode (SCE).[8] Holm et al.[9] initiated the stabilization of the low oxidation states of the Fe_4S_4 cluster by using sterically demanding trialkyl phosphine ligands, and synthesized a number of iron sulfur clusters in the all-ferrous state. However, the all-ferrous $[Fe_4S_4(PR_3)_4]^0$ cluster was identified only in solution. Attempts to isolate the cluster in pure form resulted in ligand loss and the formation of higher nuclearity clusters.[10] To prevent ligand loss, a π-acid ligand which can bind the Fe_4S_4 core through σ donation and stabilize low oxidation states by π backbonding is needed. The stabilization of the all-ferrous $Fe_4S_4^0$ core using CO resulted in an $[Fe_4S_4(CO)_{12}]$ cluster[11] containing six-coordinate iron atoms and an Fe···Fe separation of 3.47 Å (compared to 2.73 Å in reduced ferredoxin); this all-ferrous cluster is thus biologically irrelevant. Herein we report an $[Fe_4S_4(CN)_4]^{3-}$ cluster that resembles the protein $Fe_4S_4^+$ active sites geometrically and spectroscopically, and possesses $[Fe_4S_4L_4]^{2-/3-}$ (L is a mono-anionic ligand) and $[Fe_4S_4L_4]^{3-/4-}$ midpoint potentials of -0.4 and -1.38 V versus Ag/AgCl, the least negative such potentials among all synthetic analogues of the Fe_4S_4 protein active sites (For the conversion among different reference electrodes, see Table 2). These redox

[*] T. A. Scott, Prof. Dr. H.-C. Zhou
Department of chemistry and Biochemistry
Miami University
Oxford, OH 45056 (USA)
Fax: (+01) 513-529-8091
E-mail: zhouh@muohio.edu

[**] We thank Dr. Catalina Achim for Mössbauer studies, Dr. Brian Bennett for collecting and simulating the EPR spectra, and Tracy Petersen, David Collins for discussion. We also thank Miami University, the donors of the American Chemical Society Petroleum Research Fund (PRF No. 39794-G3), and the National Science Foundation (ECS-0403669) for financial support. H.C.Z. also thanks the Research Corporation for an Award (RI1188). The X-ray diffractometer is supported by the NSF (EAR-0003201).

  DOI: 10.1002/ange.200460879

potentials are less negative than expected and imply a possible new path to a biologically relevant all-ferrous $[Fe_4S_4L_4]^{4-}$ cluster, which is a goal in iron–sulfur protein analogue chemistry.

The reduction of $[Fe_4S_4Cl_4]^{2-}$ in the presence of CN^- followed by the addition of $Na(BPh_4)$ leads to the formation of $[Fe_4S_4(CN)_4]^{3-}$ (**1**; Figure 1). Cluster **1** can also be made in higher yield by using $[Fe_4S_4(PiPr_3)_4]^+$ as the starting cluster.[10] The reaction between $[Fe_4S_4Cl_4]^{2-}$ and $[Bu_4N][CN]$ gave an unidentified black solid, which showed none of the electrochemical characteristics of **1** or of the one-electron oxidized form of **1**. Thus, the substitution of the Cl^- ion for the CN^- ion needs to occur after the one-electron reduction of the $Fe_4S_4^{2+}$ core. This result is consistent with the observation that the reduction of the Fe_4S_4 core facilitates ligand substitution.[9,10]

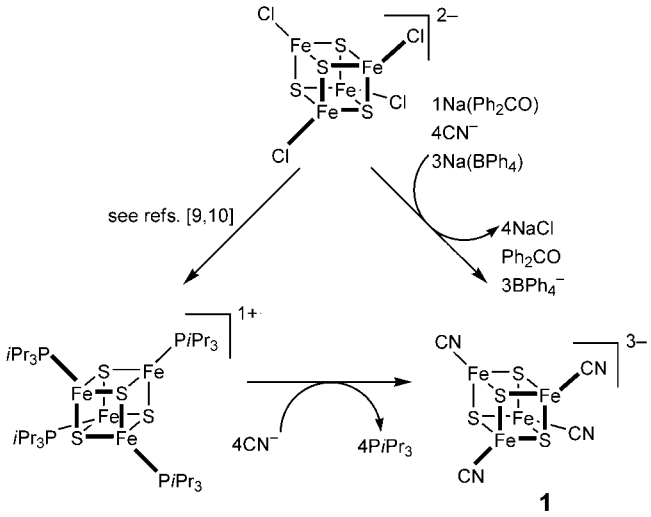

Figure 1. The preparation of the $[Fe_4S_4(CN)_4]^{3-}$ cluster **1**.

Compound **1** crystallizes in space group *R*3*c* with the N2, C2, Fe2, and S2 atoms residing on a threefold axis (Figure 2).[12] Every unit cell contains six formula units of **1**. The cluster anion has approximate T_d symmetry, but is slightly elongated along the crystallographic threefold axis. Selected interatomic distances and angles are listed in Table 1.

The Fe–S and Fe···Fe separations of **1** (Table 1) closely resemble those of the protein $Fe_4S_4^+$ core (Fe–S 2.281, 2.285; Fe···Fe 2.726 Å) in *C. acidi-urici* Fd_{red} (reduced ferredoxin),[13] and corresponding synthetic analogue $[Fe_4S_4(SPh)_4]^{3-}$ (Fe–S 2.29, Fe···Fe 2.74)[14] One of the Fe-CN groups is perfectly linear (crystallographically imposed), and the other three deviate slightly from strict linearity (Fe-C-N 174.6(3)°). An IR spectrum of **1** shows an ν(C/N) stretch at 2103 cm^{-1}, which is almost the same as the ν(C/N) stretch in $[Fe^{II}(CN)_6]^{4-}$ (2098 cm^{-1}) but quite different from that in $[Fe^{III}(CN)_6]^{3-}$ (2135 cm^{-1}), which indicates a strong π backbonding and the predominantly ferrous character of **1**.[15]

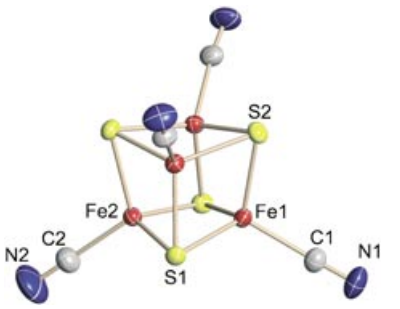

Figure 2. The structure of $[Fe_4S_4(CN)_4]^{3-}$ thermal ellipsoids set at 50% probability (see Table 1).

Table 1: Selected interatomic distances [Å] and angles [°] for **1**.

Fe···Fe	Fe–S	Fe–C	C–N	Fe-C-N
2.6906(6)	2.2791(8) 2.2846(10) 2.2863(7)	2.031(3)	1.132(4)	174.6(3)
2.7240(7)	2.3003(7)	2.016(7)	1.21(1)	180

It is informative to compare the geometric parameters of **1** with those of the recently determined crystal structure of the all-ferrous $Fe_4S_4^0$ form of the nitrogenase Fe protein from *Azotobacter vinelandii* (*Av* Fe protein).[16] The average Fe···Fe distance of 2.699 Å is slightly longer than that in the $Fe_4S_4^0$ cluster in *Av* Fe protein (2.65 Å), implying stronger Fe···Fe interaction in the all-ferrous state. In contrast, the average Fe–S separation of 2.288 Å in **1** is slightly shorter than that in the all-ferrous *Av* Fe protein cluster (2.33 Å), which reflects the elongation of the Fe–S bonds in a Fe_4S_4 cluster upon reduction from $Fe_4S_4^+$ to $Fe_4S_4^0$. This elongation of Fe–S bonds has also been observed upon the reduction of the $Fe_4S_4^{2+}$ state to the $Fe_4S_4^+$ state in other synthetic analogues.[14] The exact iron oxidation states in **1** have also been confirmed by electrochemical, EPR, Mössbauer, and UV/Vis studies.

As shown in Figure 3, the cyclic voltammogram of **1** using glassy carbon as the working electrode shows two reversible electrochemical pairs. For clarity, the redox potentials have all been converted into those versus normalized hydrogen electrode (NHE) and are listed in Table 2. In the following

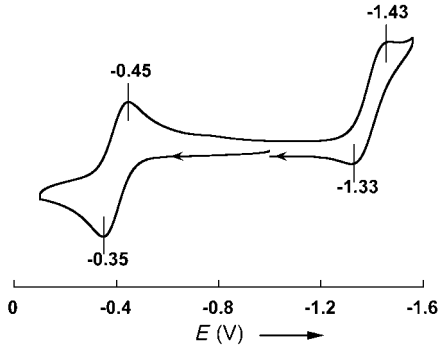

Figure 3. Cyclic voltammogram (100 $mV s^{-1}$) of $[Fe_4S_4(CN)_4]^{3-}$ in 0.1 M solution of $[Bu_4N][PF_6]$ in CH_2Cl_2. Peak potentials are those versus Ag/AgCl ($E_{1/2}$ versus Fc/Fc^+ 0.69 V; $Fc=[(C_5H_5)_2Fe]$) using a glassy carbon working electrode. Potentials versus NHE can be found in Table 2.

Table 2: Comparison of redox potentials (V) of **1** with those of the relevant Fe_4S_4 cores.[a]

L	$E_{1/2}$ $[Fe_4S_4L_4]^{2-/3-}$	$E_{1/2}$ $[Fe_4S_4L_4]^{3-/4-}$	Ref.
CN^-	−0.18	−1.16	this work
$^-SC_6H_4$-*p*-NO_2	−0.41		[19]
^-SPh	−0.76	−1.48	[8,19]
Enzyme:			
Ferredoxin	−0.4		[17]
Av Nitrogenase Fe protein		−0.8	[18]

[a] All redox potentials are those versus NHE. Standard potentials (V) in aqueous solutions at 25 °C versus NHE: SCE + 0.2415; Ag/AgCl + 0.2223.[24]

discussion, potentials are those versus NHE only. Cluster **1** possesses midpoint potentials of −0.18 and −1.16 V. The former corresponds to that of the $[Fe_4S_4L_4]^{2-/3-}$ redox pair, which is less negative than that of Fd_{ox}/Fd_{red} (−0.4 V) in native proteins;[17] the latter represents $E_{1/2}$ of the $[Fe_4S_4L_4]^{3-/4-}$ redox pair, the closest to that of iron protein of nitrogenase (−0.8 V).[18] Previously, the least negative $[Fe_4S_4L_4]^{2-/3-}$ potential in synthetic analogues was −0.41 V in $[Fe_4S_4(SC_6H_4$-*p*-$NO_2)_4]^{2-}$,[19] and that for $[Fe_4S_4L_4]^{3-/4-}$ was −1.48 V in $[Fe_4S_4(SPh)_4]^{2-}$.[8,19]

Using platinum instead of glassy carbon as the working electrode, the peak currents of **1** diminish progressively when a multiple scan is performed. Whether this is due to cyanide adsorption and polymerization on the platinum surface[20] or interaction between the clusters and the platinum surface needs further investigation.

Preliminary EPR (axial, $g_2 = 2.114$, $g_\xi = 1.897$ at 9 K) and Mössbauer (δ at 4.2 K relative to Fe metal: 0.503, 0.566; ΔE_q: 1.329, 1.869) studies have confirmed the oxidation state of **1**. The spectroscopic features are very similar to those of $Fe_4S_4^+$ proteins and their corresponding synthetic analogues,[14] but the final answer for the ground state needs high-field Mössbauer and variable-temperature EPR studies (works currently under way and will be presented elsewhere). In addition, the absorption spectrum of **1** in MeCN is featureless, in agreement with those of all other proteins and synthetic analogues in the $Fe_4S_4^+$ core oxidation state.[1]

The closest examples in the literature to **1** are the octanuclear complexes $[Fe_4S_4(NC\text{-}ML_n)_4]^{2-}$ (M = W and Mn),[21,22] where the cyanide bridges were reversed and act as linkers between an Fe_4S_4 cluster and four other metal cluster units. The core oxidation state was $Fe_4S_4^{2+}$. The key for **1** remaining monomeric is the reduction of the cluster from $Fe_4S_4^{2+}$ to $Fe_4S_4^+$. It is now possible to use **1** as a secondary building unit to clusters of higher nuclearities or coordination polymers by simply oxidizing **1** in the presence of other metal species with open coordination sites.

A monosubstituted cyanide cluster, $[Fe_4S_4(LS_3)(CN)]^{2-}$, was also detected spectroscopically,[23] but **1** represents the first all-cyanide Fe_4S_4 cluster.

In summary, we have isolated and characterized the first all-cyanide Fe_4S_4 cluster, which resembles the protein Fe_4S_4 clusters geometrically, electrochemically, and spectroscopically, and has the least negative $[Fe_4S_4L_4]^{2-/3-}$ and $[Fe_4S_4L_4]^{3-/4-}$ redox potentials among all known synthetic analogues.

Experimental Section

1 *Method A*: A black crystalline solid of $(Bu_4N)_2[Fe_4S_4Cl_4]$ (0.293 g, 0.3 mmol) was suspended in THF (2.5 mL) and mixed with a $[Bu_4N][CN]$ (0.322 g, 1.2 mmol) solution in THF (2.5 mL). Freshly made potassium benzophenoketyl (0.33 mmol) in THF (2 mL) was added drop-wise to the mixture, and the mixture was stirred for 15 min. The addition of $Na(BPh_4)$ (0.308 g, 0.3 mmol) in THF (2 mL) caused precipitation of a white solid, presumably NaCl. The resulting suspension was stirred for 1.5 h and dried under vacuum to yield a black solid. The solid was extracted with MeCN (5 mL), and the extraction was filtered through Celite. Diethyl ether vapor diffusion into the filtrate caused the precipitation of a black solid and colorless crystals within three days. The compound was purified through recrystallization from MeCN/diethyl ether with minimal amounts of MeCN to dissolve only the dark solid. Black block crystals of **1** formed after three crystallizations. Yield: 0.145 g (41 %).

Method B: A black crystalline solid of $(BPh_4)[Fe_4S_4(P\mathit{i}Pr_3)_4]$ (0.394 g, 0.3 mmol) was dissolved in THF (2.5 mL), and mixed with a $[Bu_4N][CN]$ (0.322 g, 1.2 mmol) solution in THF (2.5 mL). The mixture was stirred for 2 h to form a suspension, and then allowed to settle. The supernatant solution was decanted and the solid was washed with aliquots of THF and dried under vacuum. The black residue was dissolved in MeCN (8 mL) and crystallized from MeCN/diethyl ether yielding black block crystals of **1**. Yield: 0.240 g (67 %). Elemental analysis calcd (%) for $C_{52}H_{108}N_4Fe_4S_4$: C 52.79, H 9.20, N 8.28, S 10.84; found: C 52.57, H 9.22, N 7.98, S 10.87.

Received: June 4, 2004
Revised: July 15, 2004

Keywords: bioinorganic chemistry · cyanides · iron · nitrogenases · sulfur

[1] P. V. Rao, R. H. Holm, *Chem. Rev.* **2004**, *104*, 527 – 559.
[2] T. Herskovitz, B. A. Averill, R. H. Holm, J. A. Ibers, W. D. Phillips, J. F. Weiher, *Proc. Natl. Acad. Sci. USA* **1972**, *69*, 2437 – 2441.
[3] R. H. Holm in *Comprehensive Coordination Chemistry II*, *Vol. 8* (Eds.: J. A. McCleverty, T. J. Meyer), New York, **2004**, 61 – 90.
[4] G. D. Watt, K. R. N. Reddy, *J. Inorg. Biochem.* **1994**, *53*, 281 – 294.
[5] H. C. Angove, S. J. Yoo, B. K. Burgess, E. Münck, *J. Am. Chem. Soc.* **1997**, *119*, 8730 – 8731.
[6] B. K. Burgess, D. J. Lowe, *Chem. Rev.* **1996**, *96*, 2983 – 3011.
[7] A. C. Nyborg, J. L. Johnson, A. Gunn, G. D. Watt, *J. Biol. Chem.* **2000**, *275*, 39307 – 39312.
[8] J. Cambray, R. W. Lane, A. G. Wedd, R. W. Johnson, R. H. Holm, *Inorg. Chem.* **1977**, *16*, 2565 – 2571.
[9] C. Goh, B. M. Segal, J. Huang, J. R. Long, R. H. Holm, *J. Am. Chem. Soc.* **1996**, *118*, 11844 – 11853.
[10] H.-C. Zhou, R. H. Holm, *Inorg. Chem.* **2003**, *42*, 11 – 21.
[11] L. L. Nelson, F. Y. K. Lo, A. D. Rae, L. F. Dahl, *J. Organomet. Chem.* **1982**, *225*, 309 – 329.
[12] Crystal structure determination of **1**: $C_{52}H_{108}Fe_4N_7S_4$, $M_r = 1183.09$; a black crystal ($0.30 \times 0.27 \times 0.15$ mm) mounted on a Pyrex fiber under a cold stream of N_2, $T = 173(2)$ K, $\lambda(Mo_{K\alpha}) = 0.71073$ Å, rhombohedral, space group *R*3*c*, $a = 16.9244(3)$, $c = 38.4541$ (14) Å, $\alpha = \beta = 90°$, $\gamma = 120°$, $V = 9538.9(4)$ Å^3, $Z = 6$, $\rho_{calcd} = 1.236$ g cm^{-3}, $2\theta_{max} = 56.6°$, $\mu = 1.062$ mm^{-1}, empirical absorption correction using SADABS, $F(000) = 3822$, 22584

reflections, 3859 unique reflections, 314 parameters, 1 restraint, GOF = 1.151, $R_1 = 0.0339$ [$I > 2\sigma(I)$], w$R_2 = 0.0825$, min./max. residual electron density $-0.265/0.584$ e Å^{-3}, refined on $|F^2|$. CCDC-240511 (**1**) contains the supplementary crystallographic data for this paper. These data can be obtained free of charge via www.ccdc.cam.ac.uk/conts/retrieving.html (or from the Cambridge Crystallographic Data Centre, 12 Union Road, Cambridge CB2 1EZ, UK; fax: (+44) 1223-336-033; or deposit@ccdc.cam.ac.uk).

[13] Z. Dauter, K. S. Wilson, L. C. Sieker, J. Meyer, J. M. Moulis, *Biochemistry* **1997**, *36*, 16065 – 16073.

[14] E. J. Laskowski, R. B. Frankel, W. O. Gillum, G. C. Papaefthymiou, J. Renaud, J. A. Ibers, R. H. Holm, *J. Am. Chem. Soc.* **1978**, *100*, 5322 – 5337.

[15] K. R. Dunbar, R. A. Heintz in *Progress in Inorganic Chemistry*, *Vol. 45* (Ed.: K. D. Karlin), Wiley, New York, **1997**, pp. 283 – 391.

[16] P. Strop, P. M. Takahara, H.-J. Chiu, H. C. Angove, B. K. Burgess, D. C. Rees, *Biochemistry* **2001**, *40*, 651 – 656.

[17] J. M. Berg, R. H. Holm in *Iron-Sulfur Proteins* (Ed.: T. G. Spiro), Wiley, New York, **1982**, pp. 1 – 66.

[18] M. Guo, F. Sulc, M. W. Ribbe, P. J. Farmer, B. K. Burgess, *J. Am. Chem. Soc.* **2002**, *124*, 12100 – 12101.

[19] C. Zhou, J. W. Raebiger, B. M. Segal, R. H. Holm, *Inorg. Chim. Acta* **2000**, *300–302*, 892 – 902.

[20] G. Baltrunas, E. Morkyavichius, T. Yankauskas, *Russ. J. Electrochem.* **1998**, *33*, 572 – 575.

[21] N. Zhu, J. Pebler, H. Vahrenkamp, *Angew. Chem.* **1996**, *108*, 984 – 985; *Angew. Chem. Int. Ed. Engl.* **1996**, *35*, 894 – 895.

[22] N. Zhu, R. Appelt, H. Vahrenkamp, *J. Organomet. Chem.* **1998**, *565*, 187 – 192.

[23] R. H. Holm, S. Ciurli, J. A. Weigel, in *Progress in Inorganic Chemistry*, *Vol. 38* (Ed.: S. J. Lippard), Wiley, New York, **1990**, pp. 1 – 74.

[24] A. J. Bard, L. R. Faulkner, *Electrochemical Methods-Fundamentals and Applications*, 2nd ed., Wiley, New York, **2001**, pp. 808 – 809.

